frontiers | Frontiers in Earth Science

TYPE Original Research
PUBLISHED 14 June 2024
DOI 10.3389/feart.2024.1366156

OPEN ACCESS

EDITED BY
Eleftheria Papadimitriou,
Aristotle University of Thessaloniki, Greece

REVIEWED BY
Angelo De Santis,
National Institute of Geophysics and Volcanology (INGV), Italy
Kostas Lentas,
National Observatory of Athens, Greece

*CORRESPONDENCE
Mourad Bezzeghoud,
mourad@uevora.pt

RECEIVED 05 January 2024
ACCEPTED 13 May 2024
PUBLISHED 14 June 2024

CITATION
Ousadou F, Ayadi A and Bezzeghoud M (2024), Catalogue of source mechanisms and overview of present-day stress fields in the western region of the Africa–Eurasia plate boundary.
Front. Earth Sci. 12:1366156.
doi: 10.3389/feart.2024.1366156

Catalogue of source mechanisms and overview of present-day stress fields in the western region of the Africa–Eurasia plate boundary

Farida Ousadou[1], Abdelhakim Ayadi[1] and Mourad Bezzeghoud[2]*

[1]Centre de Recherche en Astronomie, Astrophysique et Géophysique, Algiers, Algeria, [2]Instituto de Ciências da Terra and Physics Department, Escola de Ciências e Tecnologia (ECT), University of Évora, Évora, Portugal

Complex deformation is observed along the plate boundary between the Africa and Eurasia plates, this complexity is highlighted by the faulting mechanism changing from normal faulting at the Mid-Atlantic Ridge to thrust and strike-slip faulting in the Ibero-Maghreb region (Iberia, Morocco, Algeria and Tunisia). The geodynamics of the study area shows the occurrence of NW-SE convergence between the two plates, with anticlockwise rotation. An updated scheme of the pattern of the tectonic stress direction from the Azores Archipelago to the Tunisian Atlas is presented, along with the analysis of the principal stress axis orientations ($Sh_{max} = \sigma_1$, $Sh_{min} = \sigma_3$) from the inversion of fault plane solutions. We used a catalogue of 557 fault plane solutions with only main shocks without considering the related aftershock solutions for the period from 1931 to 2020. This study complements previous work limited to Algeria and eastern Morocco by inverting earthquake mechanisms of aftershock sequences of strong events that occurred in Al Hoceima (Morocco), El Asnam, Chenoua-Tipasa, Zemmouri and Constantine (Algeria). The present work includes the area from Tunisia to the Mid-Atlantic Ridge. The inversion considers only the earthquake mechanisms of events $4.0 \leq M \leq 8.4$, excluding the aftershocks of strong events. We used the Slickenside analysis package of Michael's method. The stress field we obtained shows an extensional regime in the Mid-Atlantic Ridge, Terceira Ridge and Azores Islands and a strike-slip regime along the Gloria Fault, Gorringe Bank, and Gulf of Cadiz, to southern Spain. The same regime is also observed in the Rif and Alboran Sea. The stress regime becomes compressional in western Algeria, with strike-slip in eastern and southern Tunisia and an exception in northern Tunisia, where the stress exhibits a reverse rupture process. This study leads us to propose a new sketch of the present stress field along the western part of the Eurasia–Africa plate boundary.

KEYWORDS

source mechanisms, stress fields, western region of the Africa-Eurasia Plate boundary, inversion of focal solutions, seismicity

Introduction

The Africa–Eurasia plate boundary starts at the Azores archipelago in the Atlantic Ocean and extends to northern Tunisia, crossing the Sicilian-Calabrian arc in the Mediterranean Sea with a continuation inland in Italy to the Alps (Serpelloni et al., 2007). From the Azores triple junction to Tunisia (Figure 1), the seismicity displays a transition from a narrow seismic belt at the oceanic plate boundary in the Atlantic to a larger seismic belt area from Gibraltar to Tunisia, indicating a transition from oceanic to continental lithosphere (Jiménez-Munt et al., 2001; Buforn et al., 2004; Bezzeghoud et al., 2014).

The kinematics of the Africa plate with a fixed Eurasia were studied using Euler vectors calculated from slip vector analysis of strong earthquakes and from the trends of seafloor spreading and transform faults (Minster and Jordan, 1978; Anderson, 1985; Argus et al., 1989; DeMetz et al., 1990, 1994). The Africa–Eurasia Euler vectors combined with seismological and GPS data provide additional constraints on Africa–Eurasia plate geodynamics (Sella et al., 2002; McClusky et al., 2003; Nocquet and Calais, 2004; Serpelloni et al., 2007; Nocquet, 2012). These studies concluded that the positions of the poles are in the central Atlantic at latitudes between 20°N and 20°S. The kinematic model of Serpelloni et al. (2007) confirms the convergence direction of Africa with an anti-clockwise rotation from the triple junction to northern Libya, with an increase in velocity from 5 mm/yr to 6 mm/yr (Nocquet, 2012). The present-day kinematic model of the fixed Eurasia is highlighted by a GPS survey of the Alboran domain, the central and western parts of the Betics (southern Spain), southern Portugal, the Moroccan Rif and Atlas in Algeria. The magnitude of shortening varies from 4.5 mm/yr in the Morocco High Atlas to 5.3 mm/yr in Sicily. The 4.5 mm/yr predicted velocity in the Algerian Tell Atlas is now supported by GPS data (Bougrine et al., 2019), which provide an estimate that the velocity ranges between 4.7 and 4.9 mm/yr.

The plate kinematics were also deduced from a summation of the seismic moment of the earthquake mechanisms using the Kostrov (1974) method. This approach uses similar earthquake mechanisms considering homogeneous tectonic systems. The convergence rate, given by the orientation of the *P*-axes from the Azores Islands to the Ibero-Maghrebian region, shows a clockwise rotation, which is in agreement with the predicted directions of Africa–Eurasia convergence (Serpelloni et al., 2007; Bezzeghoud et al., 2008; Buforn, 2008; Meghraoui and Pondrelli, 2012; Nocquet, 2012; Bezzeghoud et al., 2014; Buforn et al., 2014). Bezzeghoud et al. (2014) quantified the slip derived from selected seismic events (M ≥ 5.0 shallow earthquakes) with associated earthquake mechanisms, which were compared with velocity vectors derived from kinematic models. The slip velocity values, from Bezzeghoud et al. (2014), range between 1.4 and 6.7 mm/yr, with much higher values in the Gloria Fault zone. The values are 6.7 mm/yr from the triple junction to Terceira Island, 3.1 mm/yr for the Azores Islands, 18 mm/yr for the Gloria Fault, 5.5 mm/yr for the Gorringe Bank to Cadiz, and 1.4 mm/yr for the Betics, Rif Cordillera and Alboran Sea. The convergence rate in northwestern Algeria and the Tell Atlas Mountains is approximately 3.7 mm/yr. This convergence rate is calculated based on the time span of the available earthquake database and may not be representative of the geological strain (folding and deformation). Tunisian Atlas seismicity appears to be less frequent (Figure 1), and no studies have been conducted to calculate the convergence rate from the summation of the seismic moment due to the few earthquake mechanism solutions for moderate earthquakes. Nevertheless, the predicted kinematics for the Tunisian Atlas are approximately 5.3 mm/y (Serpelloni et al., 2007).

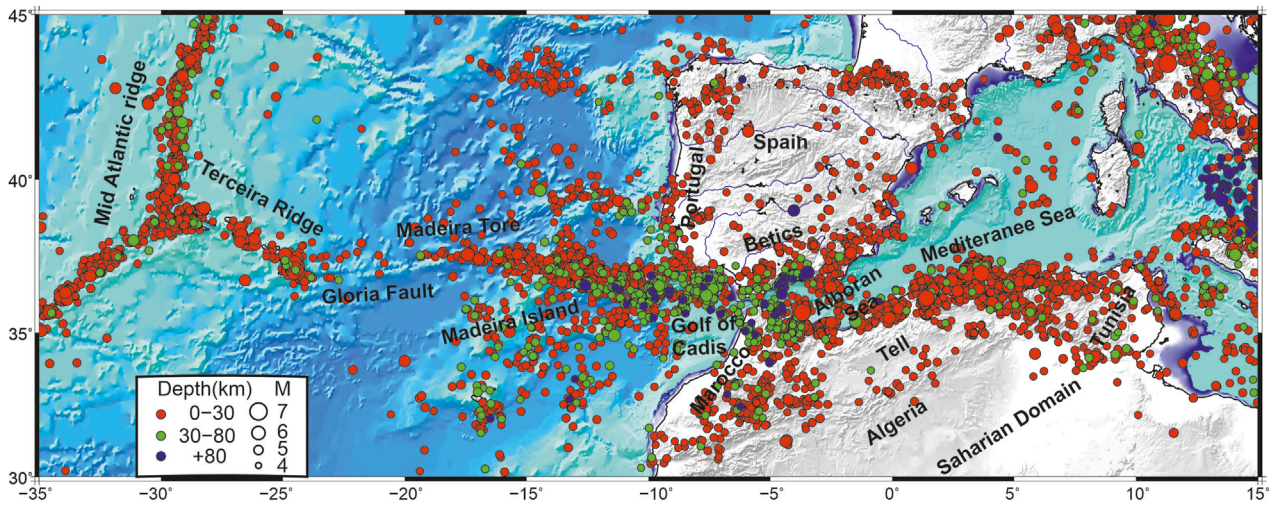

FIGURE 1
Instrumental seismicity distribution along the Africa–Eurasia plate boundary (1978–2015), with M ≥ 4 events [ISC, International Seismological Centre (2020), On-line Bulletin, http://doi.org.13.31905/D808B830]. Red, blue and green circles represent the hypocentre depths.

10.3389/feart.2024.1366156

Seismicity and faulting mechanisms in the study area

The seismicity in the study area is concentrated at shallow depths, between 5 and 30 km (the crust in the area is about 30–40 km thickness), with moderate to large magnitudes (M>7) along the boundary from the Azores triple junction to the Tunisian Atlas (Figure 1). Towards the east from the Terceira Ridge to the Gloria transform fault, the plate boundary evolves into a right-lateral tectonic regime characterised by very low magnitude and shallow-depth seismicity, except for the isolated *Ms* = 8.4 event of 25th November 1941, which occurred in the area. The transition from the oceanic to continental domains starts from the Gulf of Cadiz and extends to the Gibraltar arc, where shallow and intermediate seismicity becomes more frequent in the Gorringe Bank and Gulf of Cadiz (Figure 1). In the Betic and Alboran Seas to the northern Morocco region, seismicity is distributed nearly N–S in a large belt (~400 km), with generally intermediate seismicity clearly observed in the Alboran Sea and southern Spain, and few deep seismic events are located in southern Spain (Buforn et al., 2004, 2014, 2016). Towards the east, the seismicity is shallow and mainly distributed around the Rif Mountains in northern Morocco and in Algeria along the coastal zone within the Tell Atlas, with concentrated clusters trending NE–SW characterised by strong earthquakes (M > 6.0). The distribution of seismicity is denser in Morocco and the Tell Atlas of Algeria than in the Tunisian Atlas, which exhibits a low seismicity rate and low to moderate magnitude. Even though the seismicity of Tunisia appears to be low to moderate, damaging earthquakes have been reported to have significant surface effects (Bahrouni et al., 2014). To the south, the High Plateau seems to be characterised by very low seismicity; some sparse moderate earthquakes have been reported along the Sahara Atlas Faults system (Figure 1), whereas in the Sahara basins, seismicity has been reported mainly by seismic catalogues around the Hoggar shield, where episodic events have occurred and no other events have been observed elsewhere (Ayadi and Bezzeghoud, 2015).

From 1931 to 2020, several earthquakes with magnitudes M_s 6 and larger occurred, such as the M_w 8.2 25th November 1941, oceanic earthquake (Buforn et al., 1988a), the M_s 8.0 28th February 1969, event offshore St. Vincent Cape (Buforn et al., 1995) and the M_w 7.9 26th May 1975, Madeira earthquake (Grimison and Chen, 1986). Approximately 5 earthquakes with magnitudes of approximately 7.0, such as the M_s 7.1, 20th May 1931 Azores-Gibraltar fracture zone, the M_w 7.1, and 8th May 1939 Santa María Island (Buforn et al., 1988a); the M_s 7.1, 1 January 1980 Terceira and Graciosa Islands (Borges et al., 2007; Caldeira et al., 2017); and the M_s 7.3, 10 October 1980, El Asnam, Algeria (Ouyed et al., 1981), earthquakes were recorded. The remaining events with magnitudes of approximately 6 have occurred in the Ibero Maghreb zone, such as the Azores M_w 6.2, 09th July 1998, event (Borges et al., 2007); the M_w 6.8 21st May 2003, Boumerdès earthquake (Ayadi et al., 2008); and the Al Hoceima, M_w 6.4, 24th February 2004, event (Von der Woerd et al., 2014) (Figure 1).

The available fault plane solutions in the study area have different shapes from west to east (Figure 2A). Along the Mid-Atlantic Ridge, normal fault plane solutions follow a relatively simple model, with an E-W to ESE-WNW extensional orientation (zone 1, Figure 2A). Transform faults associated with normal and strike-slip mechanisms were identified at the Azores Archipelago, where the Mid-Atlantic Ridge meets the E–W-trending Terceira Ridge (zone 2 in Figure 2A). The strike-slip mechanism mostly prevails from the Gloria Fault to the Madeira Torre fault (zone 3 in Figure 3) (Argus et al., 1989; Geissler et al., 2010). Between the Gorringe Bank and Gulf of Cadiz (zone 4 in Figure 2A), which corresponds to the oceanic–continental transitional domain along the Africa–Eurasia plate boundary, the faults are mainly reverse at shallow depths in the Gorringe Bank and strike-slip at intermediate depths in the Gulf of Cadiz (Stich et al., 2005; Geissler et al., 2010). Along the area from the offshore Gibraltar arc to western southern Spain, shallow normal and intermediate strike-slip mechanisms with moderate magnitudes are observed (zone 5 in Figure 2A) (Medina, 1995; Fernández-Ibáñez et al., 2007). The Betics in eastern southern Spain are essentially characterised by shallow strike-slip and deep normal to trans-tensional earthquake mechanisms (zone 6 in Figure 2A) (Buforn et al., 2004, 2014, 2016; Bezzeghoud et al., 2014), with very deep strong earthquakes located in this zone. The complex surface deformation of the oceanic–continental transition cannot be explained by simple convergence between the Africa and Eurasia plates. The deep and very deep seismicity in this area is proposed to be associated with deep dynamic processes associated with residual subduction (Blanco and Spakman, 1993; Seber et al., 1996; Calvert et al., 2000; Piromallo and Morelli, 2003; Gutscher et al., 2012). The Alboran Sea domain (zone 7 in Figure 2A), located between the Betic region and the northern Rif region of Morocco, mostly features strike-slip faulting with few normal faulting mechanisms (Bezzeghoud and Buforn, 1999; Buforn et al., 2004; Gutscher et al., 2012; Bezzeghoud et al., 2014). The Rif region in northern Morocco exhibits shallow strike-slip motion (zone 8 in Figure 2A) and has experienced strong earthquakes: the Al Hoceima M_s 6.0 1994, M_w 6.4 2004 (Calvert et al., 1997; El Alami et al., 1998; Bezzeghoud and Buforn, 1999; Dorbath et al., 2005; Van der Woerd et al., 2014) and M_w 6.4 2016 earthquakes (Gràcia et al., 2019).

In addition, western Algeria, which extends from 2°W to 5°E, is one of the most active domains in the study area (zone 9 in Figure 2A). Most of the earthquake mechanisms show purely or predominantly reverse mechanism components, and very few of these mechanisms exhibit slight strike-slip motion. The region has experienced large earthquakes, such as the M_w 6.8 earthquake of 21st May 2003, associated with the southern Mitidja active reverse fault (Bounif et al., 2003; Ayadi et al., 2008; Maouche et al., 2011) and the M_s 7.3 earthquake of 10th October 1980, associated with the El Asnam active reverse fault (Philip and Meghraoui, 1983; Meghraoui et al., 1986). Northeastern Algeria and Tunisia are characterised by moderate earthquakes (Harbi et al., 1999; Bahrouni et al., 2012; Ousadou et al., 2013; Ayadi and Bezzeghoud, 2015; Soumaya et al., 2015). Most of the solutions exhibit strike-slip motion associated with the predominant strike-slip faulting in the Constantine and Guelma basins (zone 10 in Figure 2A). The southern Tunisia (zone 11 in Figure 2A) region of the Saharan Atlas is characterised by folds trending in a NW-SE direction associated with dextral and sinistral strike-slip faults (Meghraoui et al., 1986; Ben Ayed, 1993; Swezey, 1996; Bahrouni et al., 2014). Tunisia has a range of low to moderate earthquakes with magnitudes ranging from $2 \leq M \leq 5$ located in the northern part of the Gafsa region (Sïdi et al., 2011; Bahrouni et al., 2012). This shape of seismicity

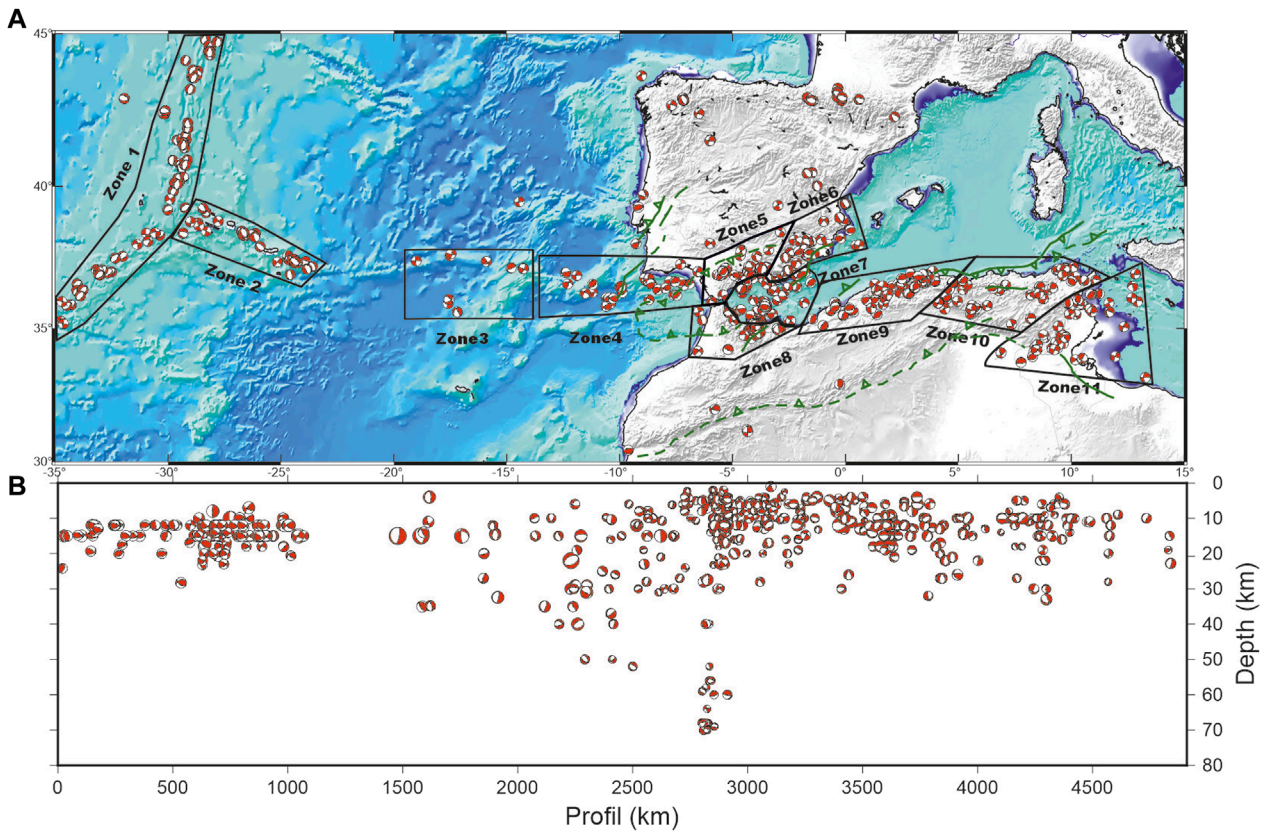

FIGURE 2
(A) Earthquake mechanisms along the Africa–Eurasia plate boundary used in this study and zoning areas. The fault plane solution parameters are listed in Supplementary Table S1, along with the mentioned references. Green lines represent the main active faults according to De Vicente et al. (2008) and from QUAFI website (http://info.igme.es/qafi/) reporting the main quaternary Active faults in Iberia and Northern Algeria. **(B)** The related cross-section of figure **(A)**.

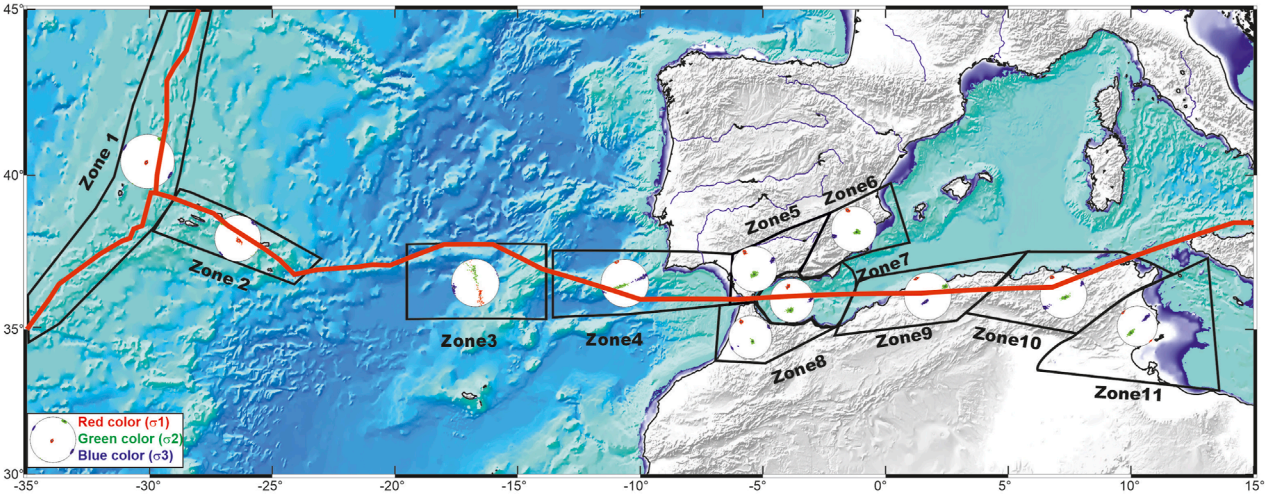

FIGURE 3
Stress tensor inversion results for the 11 seismogenic zones. The red line corresponds to the Africa-Eurasia plate boundary and the mid-Atlantic ridge. Standard deviations of each stress component for the eleven zones are given in Table 1.

and fault plane solutions are a result of a complex crustal stress pattern (Buforn et al., 1988b; Rebaï et al., 1992; Buforn et al., 2004; Vannucci et al., 2004; Bezzeghoud et al., 2014). A cross section is given by Figure 2B and shows the distribution in depth of the various earthquake mechanisms collected during our study. Most of the earthquake mechanisms are located between the surface and 30 km depth the deeper solutions are located in south Spain in the Alboran Sea.

In this work, we present an updated view of the actual tectonic (second-order) stress field following the definition of Heidbach et al. (2007, 2010) using the orientation of principal stress axes (σ1 = Sh_{max}, σ3 = Sh_{min}) calculated from earthquake mechanism inversion. We used the available catalogue of fault plane solutions of the region between the Azores Islands and Tunisia. In our inversion, we did not include the fault plane solutions related to deep earthquakes reported in the study area that occurred beyond the crust. These events are related to deep processes that took place in the lithosphere under the Betics. Unlike a previous study (Ousadou et al., 2014) that focused on the Maghreb area (Morocco and Algeria), we considered the mechanisms of only the main earthquakes without considering their related aftershock sequences. We divided the study area into 11 zones starting from the Mid-Atlantic Ridge and extending to Tunisia based on the seismicity distribution, earthquake mechanism type and consideration of the stability of the stress tensor. This study aims to provide new insights into the present-day stress state and tectonic regime, showing the spatial variation in these states from Azores to Tunisia along the plate boundary via inversion of earthquake mechanism solutions and comparisons with earlier kinematic models.

Data and resources

Available fault plane solutions were compiled from Azores to Tunisia from different published studies and completed by data from the Harvard Global Centroid Moment Tensor (see Dziewonski et al., 1981; Ekström et al., 2012), Euro-Mediterranean Regional Catalog (RCMT, Pondrelli et al., 2004, 2007, 2011), Instituto Nazionale Geofisica e Vulcanologia (INGV, 2023), ETH Zurich (ETHZ), ISC Bulletin (Lentas et al., 2019). We collected data on a total of 557 individual earthquake mechanisms from 1931 to 2020 (Figure 2) for the whole area of study, with seismic event magnitudes ranging from 4≤ M ≤8.4. All earthquake mechanisms are well distributed throughout the study area. The zoning of the study area is defined according to the similarity of the earthquake mechanisms for each zone. These zones cover the majority of the active deformed parts of the area of study. We consider large zones that contain sufficient earthquake mechanisms to assure a reliable solution of the direction of the stress regime. All the earthquake mechanisms are listed in Supplementary Table S1 with their source parameters.

Stress inversion methodology

To calculate the stress state field, we use a quantitative inversion of the fault plane solutions representing a fracture at depth. The slip vector on a fault plane during a seismic event corresponds to the stress conditions at the hypocentral depth. Over the entire thickness of the seismogenic layer, present-day tectonics are sampled by earthquake mechanisms (Arthaud, 1969).

All the methods for stress inversion require the two assumptions of Bott (1959): the first assumption is that the stress field in the study area is invariant and homogeneous in space and time; the second assumption is that the slip on a fault plane occurs in the direction of the maximum resolved shear stress. The inversion gives the mean best fitting deviatoric stress tensor using a set of slip vectors by minimising the angular deviation between the predicted and observed slip vectors of each fault plane solution. The four parameters computed in such inversions are the orientations of the principal stress axes σ1, σ2, and σ3 (with σ1> σ2> σ3) and the shape factor $R = (\sigma2 - \sigma3)/(\sigma1 - \sigma3)$ (with $0 \leq R \leq 1$), which is a linear quantity describing the relative stress magnitude.

Among all the published methods for retrieving stress field components from earthquake mechanism inversion, we select the Michael's Slickenside Analysis Package (Michael, 1984, 1987). The computation of the stress state from earthquake fault plane solutions requires selection from each pair of nodal planes and the preferred fault plane. For strong seismic events, selection is possible if a co-seismic rupture occurs or if the spatial distribution of the aftershock sequence is retrieved. For low and moderate seismic event magnitudes without surface rupture, the fault plane can be obtained via computation. Considering the ambiguity of fault plane selection, we proceed with the strategy of Ousadou et al. (2014), who retained a misfit angle (τ) less than 30° between the observed and calculated slip. We first inverted all the mechanisms for each zone to identify the misfit angle (τ). The first inversion provides an initial stress tensor using all the data to recognise mechanisms with misfits larger than 35°. The incompatible mechanisms are removed from the final inverted dataset. In the second step, the new stress tensor is calculated with only selected mechanisms without considering incompatible data. The tectonic stress regime across the entire thickness of the seismogenic layer is defined according to the orientation of the horizontal principal stresses (Sh_{max}: the σ1 maximum horizontal stress axis; Sh_{min}: the σ3 minimum horizontal stress axis). Michael's method was chosen for this study to obtain appropriate estimates of uncertainties and to increase the accuracy of noisy datasets characterised by small magnitude events (Hardebeck and Hauksson, 2001). It is important to remember that the inversion method does not consider the size of the earthquakes but only principal directions σ1, σ2 and σ3.

Inversion results

The study area was divided into eleven (11) zones starting from the Azores triple junction to the Tunisian Atlas according to the type of fault plane solution, which included those zones with similar mechanisms (Figure 2). During the inversion process, two significant cases are observed: one is related to the zone with few fault plane solutions, such as zone 3, with almost 10 mechanisms for which the tensor is easy to calculate due to the coherence of the fault plane solutions. The second case is related to zones with a large number of mechanisms with significant variations in the rupture mechanism. In this case, the tensor is also easily calculated due to the number of data points used, which allows us to keep only solutions that fit the selected criteria (Ousadou et al., 2014). In

this study, we present the calculations performed to determine the current stress by inverting all available earthquake mechanisms for each zone, and we present the best stress tensor. We emphasize here that intermediate and deep seismicity were not considered in the inversion process, especially for the Gulf of Cadiz and the Alboran Sea.

The eleven zones are illustrate by the figures numbered from Figures 4–9.

Zone 01: This zone, in the westernmost part of the study area, includes the Mid-Atlantic Ridge in the N–S direction around the Azores triple junction between the American, African, and Eurasian plates, with 117 selected mechanisms. Most of these faults are related to normal faults, and very few exhibit a small strike-slip component. All the seismicity in this zone is shallow, with depths not exceeding 10 km. This seismicity is associated with the extensional regime accompanying the opening of the Atlantic Ocean. Among the 117 faults of the Mid-Atlantic Ridge, 113 inverted mechanisms exhibit a triaxial normal regime with a clear vertical σ1 (Sh_{max}) and horizontal σ2 and σ3 at N230° and N302°, respectively, with a shape factor R of approximately 0.5 confirming the radial triaxial regime (Figure 4). The four mechanisms removed from the inversion for these zones even exhibit similar rupture mechanisms, and the misfit angle between the calculated and observed rakes is greater than our threshold of 30°.

Zone 02: The Azores archipelago is the second zone considered in this study and is composed of several islands with a low rate of seismic activity. The seismicity in this zone is characterised by a low magnitude, and most of the seismicity is related to volcanic activity. Thirty-eight mechanisms were collected for the Terceira Ridge-Azores Islands, which exhibit normal faulting for the majority of the islands, with a few others exhibiting normal faulting but with a large strike-slip component. The inversion of the total fault plane solutions give a triaxial normal stress tensor similar to that obtained in zone 1 and supported by a shape factor of approximately 0.6 with a vertical σ1 (Sh_{max}) and a horizontal σ2 and σ3 in the N317° and N277° directions, respectively. However, we observe an inversion of σ2 and σ3 regarding the tensor calculated in the Mid-Atlantic Ridge (Figure 5).

Zone 03: In this zone, only 11 strike-slip rupture mechanisms were reported from the Gloria Fault to the Madera Tore (Figure 5). Only two of these faults exhibit normal faulting with a large strike-slip component. In this zone, the 10 inverted solutions provide a low-quality result. The distribution of principal axis orientations shows a horizontal σ3 in the N257° direction, while the other two stress axes, σ1 (N338°) and σ2 (N335°), are oblique and form a continuous band across the stereo plot, indicating cylindrical symmetry of the stress state, which is consistent with a uniaxial extension regime around Sh_{min} (Figure 5) with a shape factor value of 0.7 (σ1≈σ2). Sh_{max} seems to switch gradually from the vertical to the horizontal position relative to earlier values. It is important to note the instability of the tensor due to the reduced amount of inverted data used in the process, although the nine solutions of the set exhibit good coherence.

Zone 04: We collected 32 fault plane solutions between the Gorringe Bank and Gulf of Cadiz, 29 of which were inverted (Figure 6). Most of the solutions involve strike-slip or reverse faulting mechanisms with large strike-slip components. No normal solution was observed in this area. The principal directions show a strike-slip stress regime with a good horizontal orientation of σ1 at N340°, while σ2 and σ3 (N253°) form a band, indicating cylindrical symmetry of the stress state with a uniaxial strike-slip regime around Sh_{max} (Figure 6) with a shape factor R value of 0.1 (σ2≈σ3). Beginning at this area, Sh_{max} increases in the horizontal direction, and the stress state transitions from the normal to the strike-slip regime.

Zone 05: In this zone, we collected 42 earthquake mechanisms from the Gibraltar arc to southwestern Spain. These earthquake mechanisms vary from strike-slip to normal faulting, with a large strike-slip component and pure normal to pure reverse mechanisms (Figure 6). We inverted only 22 of these earthquake mechanisms to obtain a well-constrained strike-slip stress tensor (vertical σ2) with horizontal σ1 and σ3 in the N330° and N243° directions, respectively (Figure 6). A shape factor R of 0.4 indicates a radial triaxial tensor. The remaining 20 fault solutions that were excluded from the inversion do not fit the selection criteria for the inversion process, as described in the methodology (Ousadou et al. (2014)).

Zone 06: In the southeastern Betics, 42 earthquake mechanisms were collected, most of which were strike-slip or normal mechanisms with large strike-slip components, and very few were purely normal (e.g., n°52, 366, 370) (Figure 7). Thirty-two solutions (76% of the dataset) were retained for the inversion process, and a strike-slip stress tensor (vertical σ2) is obtained with horizontal σ1 and σ3 components in the N342° and N251° directions, respectively (Figure 7). The shape factor R = 0.5 confirms the radial triaxial strike tensor. This stress is similar to that calculated for the southern western region of Iberia in zone 5.

Zone 07: The Alboran Sea domain, located between the Betics and the Moroccan Rif (Figure 7), is one of the most seismically active zones in the study area. The 63 mechanisms collected for this zone are normal or reverse and have a large strike-slip component. The 35 inverted solutions (70% of the dataset) yield a strike-slip stress tensor with oblique σ1 (N344°) and σ2 (N189°) components. Only σ3 is horizontal in the N277° direction (Figure 7). A shape factor of R=0.4 indicates a triaxial regime. Even though this tensor is similar to that calculated for the southeastern region of the Betic domain, the Sh_{max} for the Alboran Sea is not nearly horizontal (with a 35° inclination for σ1) (Figure 7).

Special attention is given to this area considering its position as a transition zone between continental and oceanic domains. Therefore, we calculate the stress tensor separately from the other areas.

Zone 08: We collected 50 mechanisms for the Rif region and inverted 41 mechanisms (82% of the dataset). Most of these mechanisms are strike-slip or normal, with large strike-slip components, and a few are reverse, with large strike components (mechanisms n°23, 375, 389) (Figure 8). The inversion leads to a good strike-slip tensor with a horizontal σ1 and σ3 in the N330° and N240° directions, respectively, and a shape factor of 0.6, reflecting a radial triaxial stress regime (Figure 8). This stress is quite similar to those calculated for southern Iberia and the Alboran Sea but with a clear horizontal σ1.

Zone 09: For the western Algerian Tell Atlas, which extends from the Algerian coastal margin to the South Atlas fault system, we collected 64 mechanisms and inverted 51 to retrieve the stress tensor (83% from the dataset) (Figure 8). This area is the most active

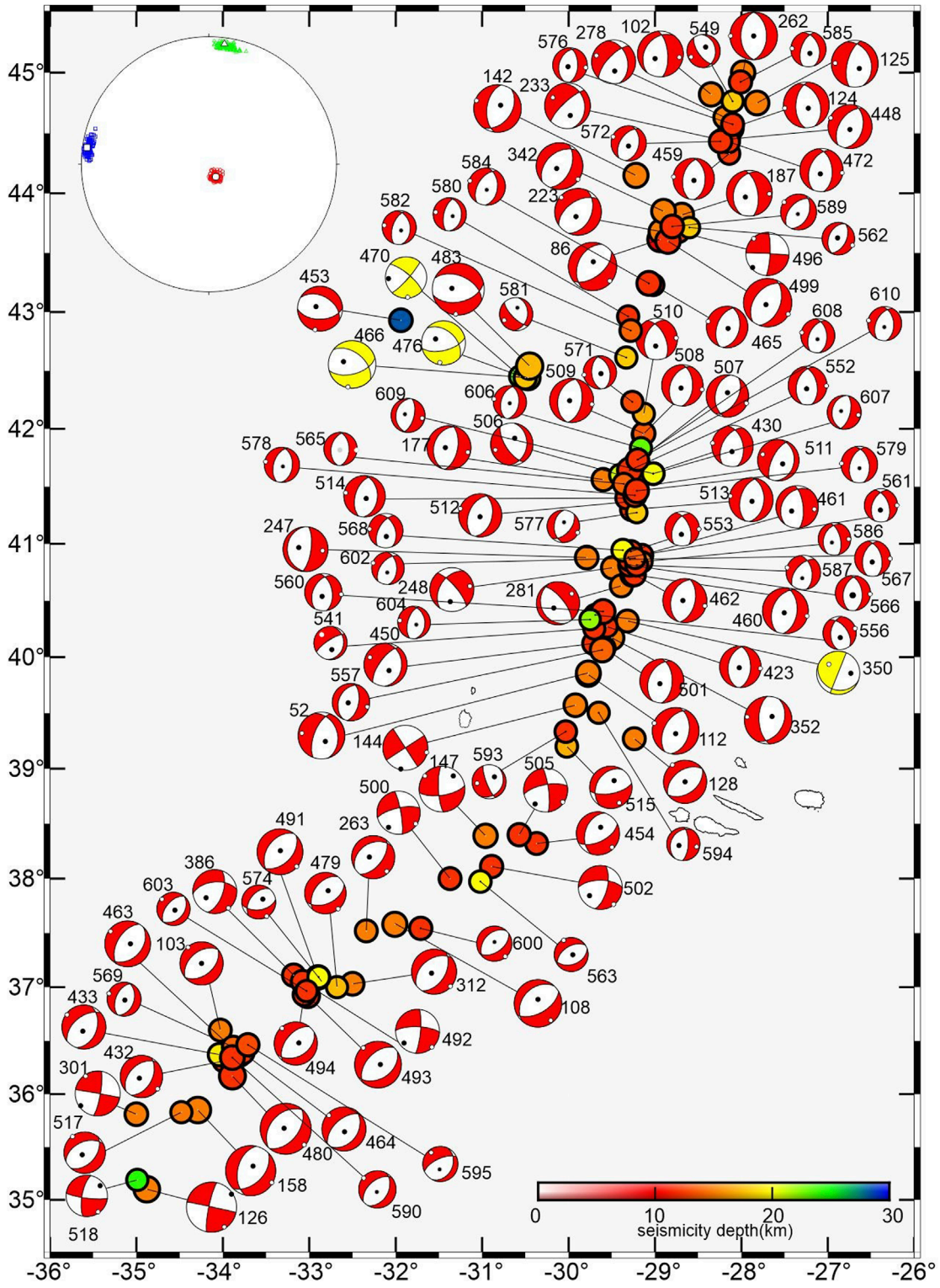

FIGURE 4
Fault plane solutions of zone 1 (the Mid-Atlantic Ridge region), with the corresponding stress tensor at the top left. σ1 is in red, σ2 is in green and σ3 is in blue. The solutions rejected by the stress inversion process are shown in yellow.

region with strong destructive earthquakes and is characterised by predominant reverse mechanisms, with some exhibiting a small strike component. Very few strike-slip or normal strike-slip mechanisms exist. The inversion of the selected mechanisms reveals a pure reverse stress tensor with σ3 in the vertical direction and σ1 and σ2 in the horizontal direction at N327° and N241°, respectively

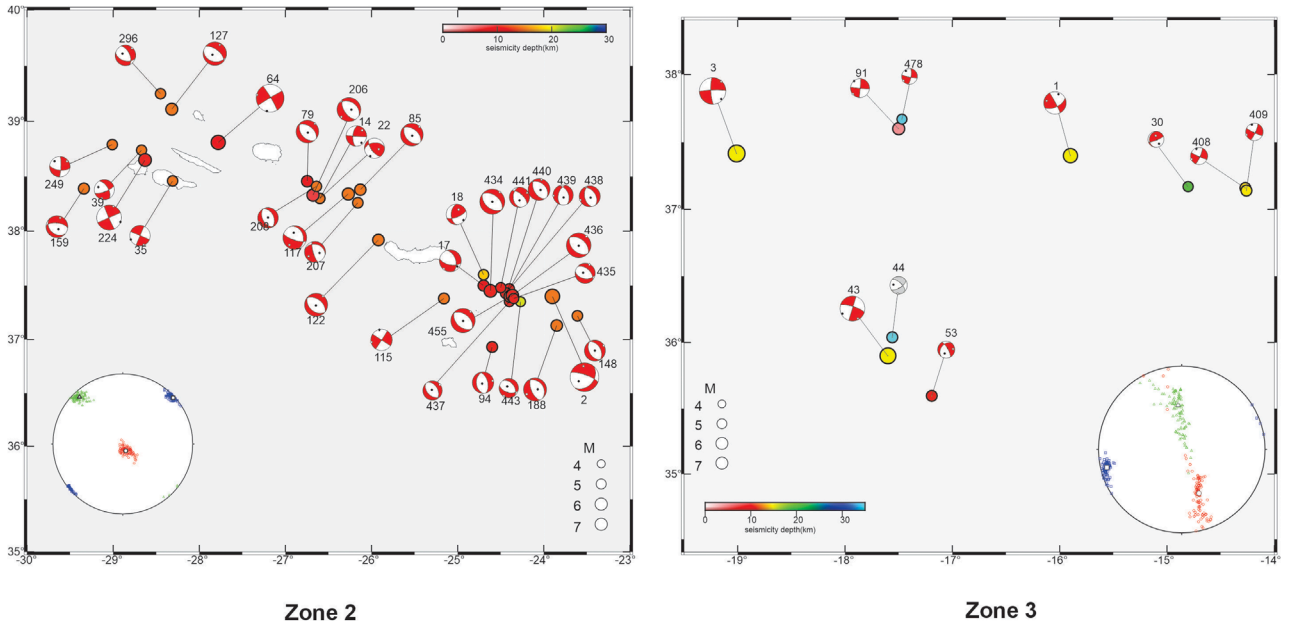

FIGURE 5
Fault plane solutions of zone 2 (the Terceira Ridge-Azores Island) and zone 3 (the Gloria Fault-Madera Tore region), with the corresponding stress tensor in the bottom left and right respectively. σ1 is in red, σ2 is in green and σ3 is in blue. The solutions rejected by the stress inversion process are shown in grey.

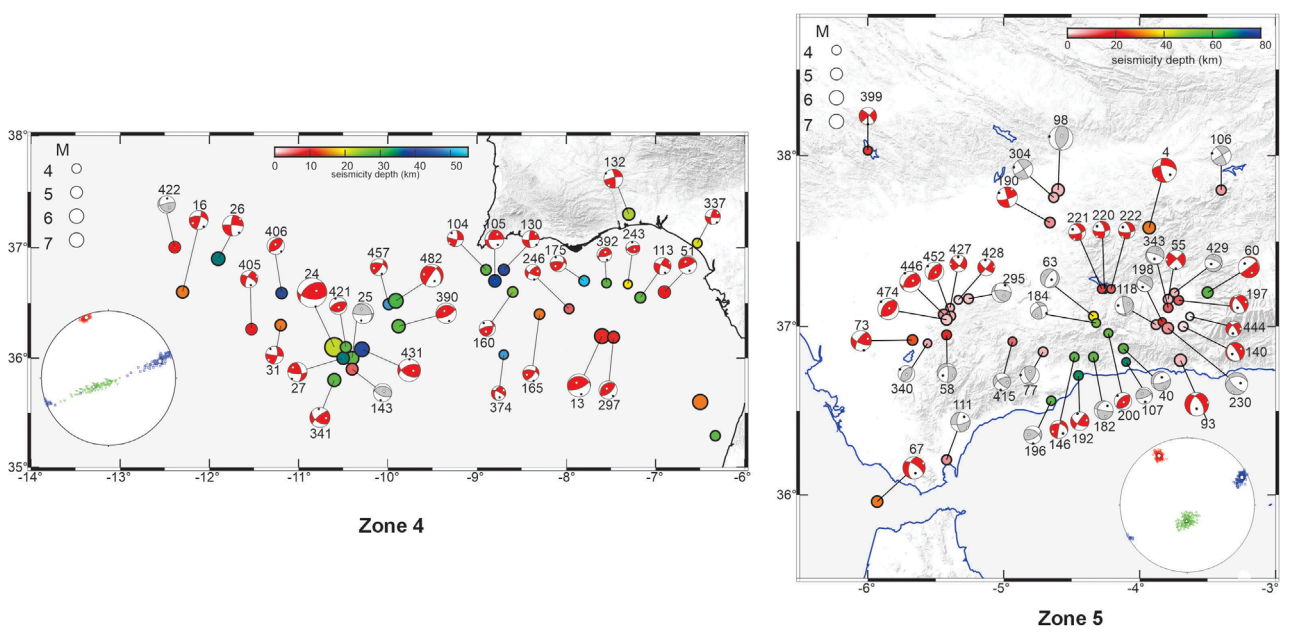

FIGURE 6
Fault plane solutions of zone 4 (the Gorringe Bank to Gulf of Cadiz region) and zone 5 (the offshore Gibraltar arc to the southern west of Spain), with the corresponding stress tensor on the left top and bottom right respectively. σ1 is in red, σ2 is in green and σ3 is in blue. The solutions rejected by the stress inversion process are shown in grey.

(Figure 8). A shape factor of approximately 0.4 indicates a triaxial tensor.

Zone 10: Eastern Algeria and northern Tunisia are located on the northern edge of the Maghrébides chain. Unlike the other intermountain basins of the western part of the Tell Atlas, the eastern Algeria basins were uplifted during Quaternary collision processes, similar to those of Constantine and Guelma, which exhibit relatively high elevations (1,060 m). We selected 53 earthquake mechanisms and retained 38 of them in the final inversion (84% of the dataset). The computed stress tensor shows a clear strike-slip stress

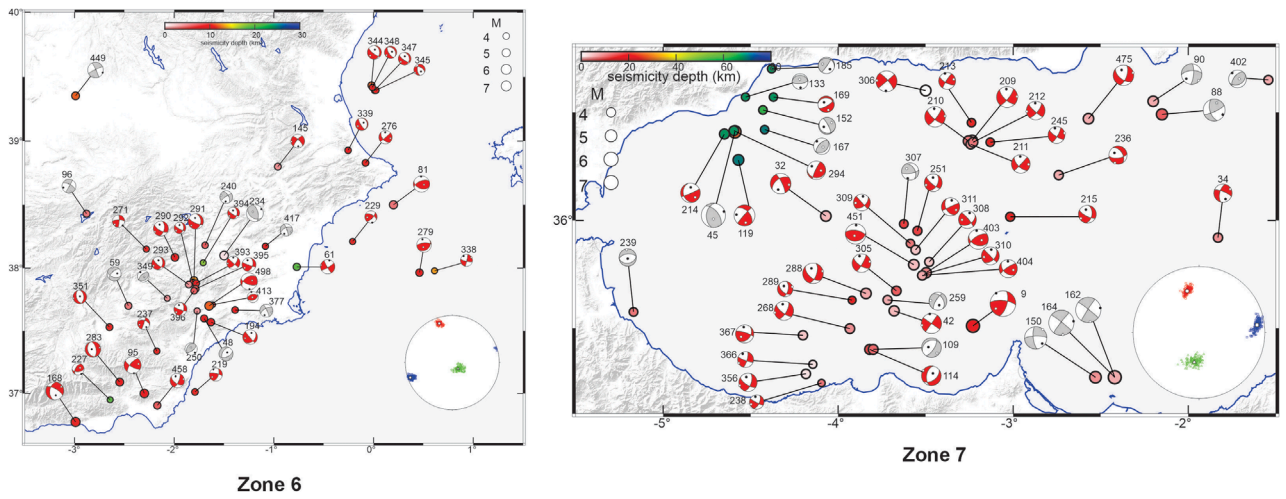

FIGURE 7
Fault plane solutions of zone 6 (southeast of the Betics) and zone 7 (the Alboran Sea domain), with the corresponding stress tensor on the bottom right. σ1 is in red, σ2 is in green and σ3 is in blue. The solutions rejected by the stress inversion process are shown in grey.

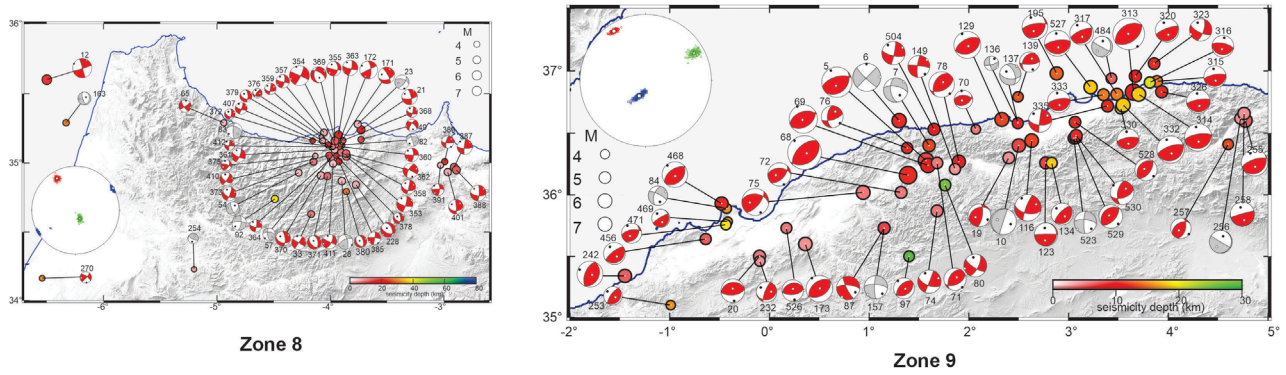

FIGURE 8
Fault plane solutions of zone 8 (the Rif region) and zone 9 (the western Algerian Tell Atlas), with the corresponding stress tensor on the bottom left and top left respectively. σ1 is in red, σ2 is in green and σ3 is in blue. The solutions rejected by the stress inversion process are shown in grey.

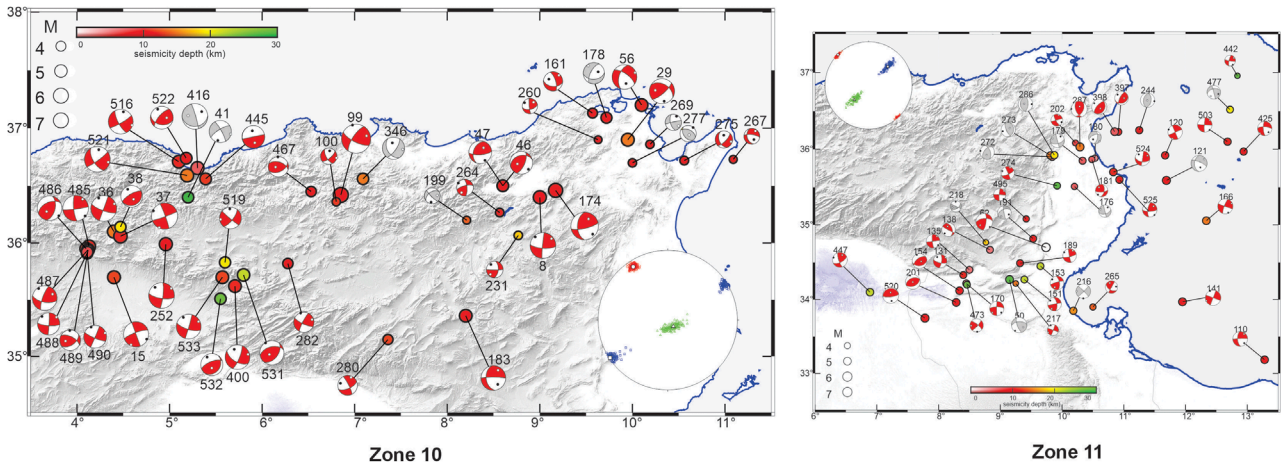

FIGURE 9
Fault plane solutions of zone 10 (eastern Algeria and northern Tunisia) and zone 11 (east-south Tunisia), with the corresponding stress tensor on the bottom right and top left respectively. s1 is in red, s2 is in green and s3 is in blue. The solutions rejected by the stress inversion process are shown in grey.

TABLE 1 Stress tensors principal components with their standard deviation, obtained by inversion for the 11 zones in the western part of the Africa–Eurasia plate boundary from the Azores triple junction to the Tunisian Atlas. For more details, see the text.

Zones	Azimuth/Plunge (in degree)					Δσ3(°)	R	Number of solution used / Total number of dataset
	σ1(°)	Δσ1(°)	σ2(°)	Δσ2(°)	σ3(°)			
Zone 01	—	—	N212/04	±4	N302/01	±9	0.5	113/117 (96%)
Zone 02	—	—	N317/09	±7	N277/02	±9	0.6	38/38 (100%)
Zone 03	N338/43	±5	—	—	N257/08	±15	0.7	10/11 (90%)
Zone 04	N340/04	±3	—	—	N253/20	±2	0.1	29/32 (90%)
Zone 05	N330/16	±5	—	—	N243/10	±5	0.4	22/42 (52%)
Zone 06	N342/13	±2	—	—	N251/06	±2	0.5	32/42 (76%)
Zone 07	N344/35	±7	N189/52	±20	N277/12	±10	0.4	35/63 (70%)
Zone 08	N330/17	±3	—	—	N240/01	±3	0.6	41/50 (82%)
Zone 09	N327/12	±3	N241/16	±4	-	-	0.4	51/64 (83%)
Zone 10	N327/10	±3	—	—	N237/01	±3	0.3	38/53 (84%)
Zone 11	N316/01	±3	—	—	N226/38	±2	0.3	30/45 (68%)

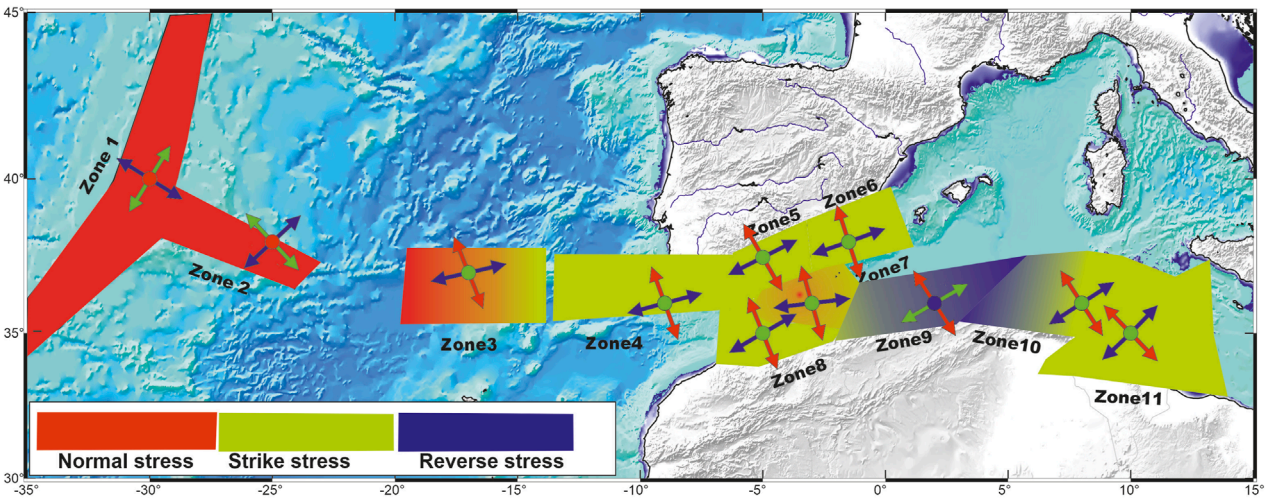

FIGURE 10
Spatial variation in the current stress regime deduced from this study. Red colour for extensional regime (normal stress), green colour for transcurrent regime (strike slip stress), and blue colour for compressional regime (reverse stress). The arrows and dotes correspond to the principal stress components [σ1 (red), σ2 (green) and σ3 (blue)].

regime with horizontal σ1 and σ3 trending in the N327° and N237° directions, respectively (Figure 9). The shape factor R is approximately 0.3, indicating a triaxial stress tensor.

Zone 11: In eastern Tunisia from the north to the Gulf of Gabès to the southeastern region, the majority of the collected fault plane solutions were found to have predominant strike-slip mechanisms, with few solutions exhibiting reverse mechanisms with a strike-slip component. The inversion of the 30 selected earthquake's mechanisms among 45 that were collected (70% of the dataset) gives a strike-slip stress tensor with a clear horizontal σ1 in the N316° direction and a nearly horizontal σ3 in the N226° direction (Figure 9). A shape factor R of approximately 0.3 indicates that σ2 is near σ3.

Discussion

In this study, we calculated stress tensors by inverting earthquake's mechanisms to highlight the current tectonic regime along the boundary between the Africa–Eurasia plates from the

Azores Archipelago to northern Tunisia, highlighting its spatial variation. We have used all the available earthquake solutions, from ISC database and other scientific studies, in each eleven zones we considered in the study area. Extension, strike-slip and reverse rupture mechanisms were found and are well defined in most areas with high values.

Along the Mid-Atlantic Ridge area, where the three major tectonic plates intersect, we obtained a good radial extension stress along the Mild Atlantic and Terceira Ridges (zone 1, Figure 3) and on Azores Island (zone 2, Figure 3) with permutations of the positions σ2 and σ3 (Fig. 03); however, left-lateral strike-slip motion was found in the Terceira Ridge by Bezzeghoud et al. (2014) via the total seismic moment tensor summation method. The seismicity in the Mid-Atlantic to Terceira Ridges is related to seafloor spreading (Argus et al., 1989; Demets et al., 1990; Jimenez-Munt et al., 2001; Buforn et al., 2004) when the seismicity of the Azores Islands was associated with the North American and African plate boundaries. The tectonic stress changes towards the east across the Gloria fault and Madera Tore area (zone 03, Figure 3), where the seismicity level seems to be very low, and the Gloria Fault is considered seismically inactive with no recent moderate seismic events (Buforn et al., 1988a; Bezzeghoud et al., 2014). Nevertheless, within this region, a significant change in the tectonic regime occurs from a purely radial extensional stress regime (vertical Sh_{max}) to a uniaxial shear-normal stress regime, as also reported by De Vicente et al. (2008) and Bezzeghoud et al. (2014). The tectonic regime is more strike-slip from the Madera Tore to the Gulf of Cadiz, crossing the Gorringe Bank (zone 04; Figure 3) with a clear horizontal Sh_{max} in the N340° direction, where Bezzeghoud et al. (2014) determined a reverse regime and De Vicente et al. (2008) found a uniaxial reverse regime, the latter of which uses only 05 mechanisms. The current regime in southern Spain features a clear triaxial strike (zones 05 and 06; Figure 3), which is the same as that calculated for the Rif in northern Morocco (zone 08; Figure 3), with a pure horizontal Sh_{max}, which agrees with the pure strike-slip given by De Vicente et al. (2008) and Bezzeghoud et al. (2014), including the Alboran Sea area. The regime we calculated for only the Alboran Sea (zone 07; Figure 3) exhibits a uniaxial normal regime with a strike-slip component and an oblique Sh_{max}. The Alboran Sea is a key region that is still under debate, with numerous models proposed to interpret the uplift of the Betic (zones 5 and 6) and Rif (zone 08) ranges and the subsidence of the Alboran Sea (zone 07) (Platt and Vissers, 1989; Watts et al., 1993; Seber et al., 1996; Andeweg and Cloetingh, 2001; Koulali et al., 2011; Martinez-Garcia et al., 2011). Across the Iberian Peninsula, Using Reches's method, De Vicente et al. (2008) have used 213 earthquake mechanisms to calculate the stress state.

Considering the local tectonic processes in the Iberian region, the Alboran Sea and the Rif Mountains with intermediate seismicity in the Alboran Sea, intermediate to deep seismicity in the southwestern region of Spain and shallow seismicity in the Betic and Rif regions, we decided to also invert the intermediate depth earthquake mechanisms separately from the others. Thus, we found a pure strike-slip mechanism in the Betic and Rif regions and a normal mechanism in the Alboran Sea, in agreement with what was reported by Buforn et al. (2004) and Bezzeghoud et al. (2014).

A compressional triaxial tectonic regime is found in this study for western Algeria (zone 09 in Figure 3), as also reported by Bezzeghoud et al. (2014) and calculated from the seismic moment tensor summation (SMT); moreover, a uniaxial compressional regime was proposed by De Vicente et al. (2008). This discrepancy is probably due to the number of data points and to the selection criteria fixed in our calculation; ten mechanisms were rejected from our inversion because they do not fit the criteria that we considered.

Crossing the Tell Atlas from western to eastern Algeria, the tectonic regime changes from a compressive triaxial regime to a strike triaxial regime (zone 10 in Figure 3), in agreement with the results calculated by Ousadou et al. (2013, 2014) and largely the same as those found by Soumaya et al. (2015). Thus, between the Terceira Ridge and the Gulf of Cadiz, the stress varies gradually from triaxial extension to uniaxial compression. In the Betic–Alboran–Rif zone and in northern Algeria, the stress varies from uniaxial extension to uniaxial. Ousadou et al. (2014) calculated the stress regime across the Maghreb by inverting fault plane solutions of the largest earthquakes with their related aftershocks that occurred from northern Morocco to eastern Algeria. A total of 632 earthquake mechanisms were compiled and inverted using Michael's code (Michael, 1984, 1987) to calculate the stress tensor. A compressive stress regime was found in the Cheliff and Zemmouri seismogenic zones in central Algeria. However, a strike-slip regime was observed in eastern Algeria and in the Moroccan Rif. They concluded that the Ionian slab and the dynamics of the Alboran Sea seemed to have influenced these different regimes.

The tectonic regime in southeastern Tunisia (zone 11 in Figure 3) is a uniaxial transpressional stress regime similar to the results obtained by Soumaya et al. (2015). Soumaya et al. (2018) proposed a scheme for determining the stress field and tectonic regime in the easternmost part of Algeria to Tunisia from the inversion of fault plane solutions. They inverted 123 fault plane solutions using Frohlich's triangle to classify the type of fault plane solutions and determine the tectonic stress field (Frohlich, 1992). These data show lateral variations in the present stress regime, as shown by Heidbach et al. (2010), which is consistent with the neotectonic stress field determined using fault slip data.

The present tectonic activity and kinematics of the study area are controlled by the Africa–Eurasia plate convergence, which is influenced by lateral slab migration and by deep dynamic processes represented by lithosphere–mantle interactions in the Calabrian Arc and Alboran Sea (Ousadou et al., 2014; Soumaya et al., 2015). The NW-SE convergence direction of the African plate, with a rate of ~0.5 mm/yr towards Eurasia, is accommodated substantially in the Maghreb area (Serpelloni et al., 2007) and in the southern Tyrrhenian region (Nocquet, 2012). The general trend revealed by several studies shows an orientation of maximum horizontal stress (Sh_{max}) in the NW-SE to N-S directions. Imaging the variation in the current stress field along the boundary between the Africa and Eurasia plates will help to better explain how the fracture process occurred in each seismogenic zone from Azores to Tunisia along the boundary zone. The inversion of fault plane solutions leads us to image the fluctuation of the stress regime, starting from transtensional in the Azores Archipelago to strike-slip between the Gloria, Terciera, Gulf of Cadiz, and Alboran regions, to compressional in the western to central Algeria; in eastern Algeria and Tunisia, the stress transitions to strike-slip mode. The orientation of the horizontal axis (Sh_{max}) deduced from the inversion of earthquake mechanisms for the whole area is in agreement with the direction of plate convergence given by

several studies (Serpelloni et al., 2007; Nocquet and Calais, 2012; Bezzeghoud et al., 2014). The NW-SE direction of Sh_{min} in zone 1 is in agreement with the results obtained from morphological observations along linear volcanic ridges, where Lourenço et al. (1998) obtained the same orientation as that obtained from the Nuvel-1A model (DeMets et al., 1990). The NE-SW Sh_{min} orientation found on the Terceira Ridge and Azores Islands is similar to that of Bezzeghoud et al. (2014), and it continues in the same direction up to the Madera Tore. Between the Gorringe Bank and the Gulf of Cadiz, the kinematic behaviour changes, and Sh_{max} exhibits a horizontal direction at N340° (NNW-SSE). Crossing from southwestern to southeastern Spain, Sh_{max} changes from N334° to N343°, becoming N345° in the Alboran Sea and N335° in the Rif. In western Algeria, Sh_{max} is mostly N327°. In eastern Algeria, it becomes N334°; in northern Tunisia, Sh_{max} is N324°; and it becomes N321° in the southern region.

To date, the region at the boundary between the African and Eurasian plates has contained a dense global positioning system (GPS) network, especially in the Maghreb area (Morocco, Algeria and Tunisia). All the studies prior to the installation of these GPS networks concluded that the Africa–Eurasia convergence direction is characterised by an anti-clockwise rotation as the velocity decreases (Nocquet and Calais, 2004; Nocquet, 2012). The plate boundary consists of very well-defined lines in the Atlantic Ocean from the Azores Archipelago to 12°W. From 12°W to Tunisia, the boundary becomes more diffuse as the area becomes wider and more deformed (Buforn et al., 2004; Borges et al., 2007; Bezzeghoud et al., 2014). This boundary zone highlights the current plate movement, which is transtensional in the Azores Archipelago, dextral at the Gloria transform fault and convergent between the Gibraltar Strait and the Ibero-Maghrebian region.

Conclusion

During this study, we achieved two objectives: first, we constructed an earthquake mechanisms database containing 557 events with corresponding focal parameters from various published studies and seismological agencies. The second goal was to divide the study area into zones according to the homogeneity of the related earthquake mechanisms to calculate the stress tensor by inverting the fault plane solutions of the selected zones from the Azores triple junction to Tunisia. We inverted only 439 events from the total dataset after excluding the deep events and considering only the shallow and intermediate depth events, which were distributed as follows: 113 events in the Mid-Atlantic Ridge, 38 in the Azores Archipelago, 10 in the Gloria-Madera region, 29 in the Gorringe Bank to the Gulf of Cadiz, 22 in Gibraltar Arc-southwestern Spain, 32 in the southeastern region of the Betics, 35 in the Alboran Sea, 41 in the Rif region (Morocco), and 51 in the western-central-Tell Atlas (Algeria). Thirty eight (38) solutions in the eastern Algeria to Tunisia region and 30 in the northeastern-southeastern region of Tunisia were collected during our study (Table 1). The calculated stress field and imaging of its variation along the Africa–Eurasia plate boundary were obtained by inverting the fault plane solutions using the procedure of Ousadou et al. (2014).

The determination of the stress field by inverting fault plane solutions is obtained considering the assumption that the stress field is homogenous in space with a misfit angle of 30°. The directions of σ1, σ2 and σ3 were calculated for the 11 zones of the study area. In both the Mid-Atlantic Ridge and the Azores Archipelago, the regions are characterised by extensional movements associated with normal stresses (vertical σ1, horizontal σ2 and σ3) with a shape factor of R = 0.5–0.6 corresponding to a triaxial regime. Considering the tectonic context, σ2 and σ3 are permuted. From the Gloria fault to Madera Torre, the stress regime changes to quasi-strike-slip stress, with σ1 being horizontal and σ2 being close to vertical, with a shape factor R = 0.7, indicating uniaxial extension. From the Gorringe Bank to the Gulf of Cadiz, σ1 becomes horizontal, and σ2 becomes vertical, corresponding to a strike-slip stress regime. Here, we have a clear change in the stress regime from extensional in the western part of the study area to strike-slip stress in the Gorringe Bank-Gulf of Cadiz. In the Rif of Morocco and southern Betics, the region exhibited strike-slip stress, as shown in Figure 3. In the Alboran Sea, the stress component is not very well defined because σ1 and σ2 are oblique, and the area seems to experience a balance of stress between the normal and strike-slip directions. The stress regime changes to reverse in northwestern Algeria, with a vertical σ3, and a horizontal σ1 and σ2, with a shape factor of R=0.4, indicating a triaxial tensor. For the easternmost part of the study area, Algeria and Tunisia (zone 10), and southeastern Tunisia (zone 11), the results show a strike-slip stress with a shape factor of approximately R=0.3, indicating a revolution of σ2 and σ3 around σ1. From the Gorringe Bank to eastern Tunisia, Sh_{max} (σ1) becomes horizontal in nearly the WNW-ESE direction, except in the Alboran Sea, where σ1 is not completely horizontal due to the complexity of the region and because the Alboran microplate seems to have independent movement driven by slab rollback, as reported by Gutscher et al. (2012). The stress observed in the Alboran Sea seems to be associated with the geodynamics of this region. A present-day GPS survey reveals a displacement field in the western Alboran block (Nocquet, 2012) interpreted to be because of the presence of a microplate due to the complex geology of the region. New GPS results in the Tell Atlas of Algeria confirm the predicted 4.5 mm/yr velocity by Bougrine et al. (2019), who estimated the velocity to range between 4.7 and 4.9 mm/yr. We are now waiting for the results of GPS campaigns launched in Tunisia in 2014. The present-day tectonics have strong implications for understanding the strain pattern in the western Mediterranean region.

In conclusion, this study highlights the inhomogeneous variation in stress along the plate boundary zone from the Mid-Atlantic Ridge (extensional stress), Azores Archipelago (normal), Gloria Fault (normal strike-slip), and Gorringe Bank-Gulf of Cadiz-Betics (strike-slip), with another branch extending from the southeastern Betics to the Rif Mountains (strike-slip). In Algeria, the stress becomes compressional from the western part to the central Tell Atlas. In the eastern Tell Atlas (Algeria) to Tunisia, the stress becomes strike-slip across the whole area. On both sides of the Maghreb region, the stress regime is affected by the complex geodynamics of the Tyrrhenian and Alboran seas. This study aimed to extend the study of the variation in the stress field considering the seismicity of selected seismogenic zones from earthquake mechanism inversion beyond the region previously explored by Ousadou et al. (2014) to Tunisia, Iberia, and the Alboran Sea to the Mid-Atlantic Ridge. Our results provide answers to questions raised by Ousadou et al. (2014) about the stress tensor in Tunisia

and show that the stress in this area (zone 11) is purely strike-slip with a horizontal σ1 (N316°). The examination of the variation in the stress tensor from Tunisia to the Mid-Atlantic Ridge promotes the NW oblique convergence of the Africa–Eurasia plates and reveals a clockwise rotation of σ1 from Tunisia (zone 11) to Gloria-Fault-Madera Torre (zone 3) (Supplementary Table S1). Further west, σ1 becomes vertical (zones 1 and 2). This study leads us to conclude that the variation in the stress tensor depends on the type of data (seismic event mechanism) used. As reported by Ousadou et al. (2014), the stress tensor is locally influenced in the Tell Atlas of Algeria by the integration of the aftershock fault plane solutions in the inversion process, and a counter-clockwise rotation of σ1 is clearly demonstrated due to the local tectonic regime. In this study, when considering only the seismicity with M ≥ 4.0 from 1931 to 2020 and excluding the aftershock mechanisms during the inversion process, we found a clockwise rotation of σ1 from east to west across the Maghreb region; the same result was obtained by Soumaya et al. (2018), who reported similar values of σ1. Westwards of the study area (from the Gloria fault to the Mid-Atlantic Ridge), the principal σ1 stress component tends to be vertical, which explains the mix of strike-slip and normal faulting in this area. The present-day stress pattern is highlighted by mapping the variation in σ1 across the study area (Figure 10), dominated by the geodynamic process of the oblique NW-SE to NNW-SSE convergence of the Africa–Eurasia plates. This paper provides updated insight into the state of the stress pattern along the plate boundary zone between the Azores triple junction and Tunisia.

Data availability statement

The original contributions presented in the study are included in the article/Supplementary Material, further inquiries can be directed to the corresponding author.

Author contributions

FO: Writing–original draft. AA: Writing–original draft. MB: Supervision, Funding acquisition, Writing–review and editing.

Funding

The authors declare that financial support was received for the research, authorship, and/or publication of this article. This study was conducted within the MEDYNA FP7-PEOPLE-2013-IRSES project, WP-1: Present-day Kinematics and Seismic Hazards, funded by the Seventh Framework European Programme. This work was carried out as part of the research activities of the Centre de Recherche en Astronomie, Astrophysique et Geophysique (CRAAG, Algiers) and the Instituto de Ciências da Terra - UIDB/04683/2020 (https://doi.org/10.54499/UIDB/04683/2020).

Acknowledgments

The authors would like to thank Sofiane Gherbi and Khadidja Abbes for their help and the reviewers for their fruitful comments that improved the quality of the manuscript.

Conflict of interest

The authors declare that the research was conducted in the absence of any commercial or financial relationships that could be construed as a potential conflict of interest.

The authors declared that they were an editorial board member of Frontiers, at the time of submission. This had no impact on the peer review process and the final decision.

Publisher's note

Supplementary material

The Supplementary Material for this article can be found online at: https://www.frontiersin.org/articles/10.3389/feart.2024.1366156/full#supplementary-material

References

Anderson, H. J. (1985). *Seismotectonics of the western mediterranean*. Cambridge, United Kingdom: University of. PhD thesis.

Andeweg, B., and Cloetingh, S. (2001). Evidence for an active sinistral shear zone in the western Alboran region. *Terra nova.* 13, 44–50. doi:10.1046/j.1365-3121.2001.00314.x

Argus, D. F., Gordon, R. G., DeMets, C., and Stein, S. (1989). Closure of the Africa-Eurasia-North America plate motion circuit and tectonics of the Gloria fault. *J. Geophys. Res. Solid Earth* 94 (B5), 5585–5602. doi:10.1029/jb094ib05p05585

Arthaud, F. (1969). Methode de determination graphique des directions de raccourcissement, d'allongement et intermediaire d'une population de failles. *Bull. Soc. Geol. Fr.* 7 (XI), 729–737. doi:10.2113/gssgfbull.s7-xi.5.729

Ayadi, A., and Bezzeghoud, M. (2015). Seismicity of Algeria from 1365 to 2013: maximum observed intensity map (MOI2014). *Seismol. Res. Lett.* 86, 236–244. Number 1 January/February 2015. doi:10.1785/0220140075

Ayadi, A., Dorbath, C., Ousadou, F., Maouche, S., Chikh, M., Bounif, M. A., et al. (2008). Zemmouri earthquake rupture zone (Mw 6.8, Algeria): aftershocks sequence relocation and 3D velocity model. *J. Geophys. Res. Solid Earth* 113 (B9), B09301. doi:10.1029/2007JB005257

Bahrouni, N., Bouaziz, S., Soumaya, A., Ben Ayed, N., Attafi, K., El Ghali, A., et al. (2014). Neotectonic and seismotectonic investigation of seismically active regions in Tunisia: a multidisciplinary approach. *J. Seismol.* 18, 235–256. doi:10.1007/s10950-013-9395-y

Bahrouni, N., Soumaya, A., Ben Ayed, N., Bouaziz, S., Attafi, K., and Rebaï, N. (2012). "Investigation of historical seismicity in Tunisia from the records of building damage," in The Large Mediterranean Earthquakes from Past to Present-International Symposium, Alger, 21–23 May 2013. Abstracts vol.

Ben Ayed, N. (1993). Evolution Tectonique de l'Avant-pays de la Chaîne Alpine de Tunisie du Début du Mésozoïque à l'Actuel, Ann. Mines et Géol. *Tunisie* 32, 286.

Bezzeghoud, M., Adam, C., Buforn, E., Borges, J. F., and Caldeira, B. (2014). Seismicity along the Azores-Gibraltar region and global plate kinematics. *J. Seismol.* 18, 205–220. doi:10.1007/s10950-013-9416-x

Bezzeghoud, M., Borges, J. F., Caldeira, B., Buforn, E., and Udias, A. (2008). "Seismic activity in the Azores Region in the context of the western part of the Eurasia–Nubia plate boundary," in International Seminar on Seismic risk and rehabilitation on the 10th Anniversary of the July 9 1998 Azores Earthquake, Horta-Azores, 9–13 July 2008, 27–31.

Bezzeghoud, M., and Buforn, E. (1999). Source parameters of the 1992 Melilla (Spain,*MW*= 4.8), 1994 Alhoceima (Morocco,*MW*= 5.8), and 1994 Mascara (Algeria,*MW*= 5.7) earthquakes and seismotectonic implications. *Bull. Seismomolgical Soc. Am.* 89 (2), 359–372. doi:10.1785/bssa0890020359

Blanco, M. J., and Spakman, W. (1993). The P-wave velocity structure of the mantle below the Iberian Peninsula: evidence for subducted lithosphere below southern Spain. *Tectonophysics* 221, 13–34. doi:10.1016/0040-1951(93)90025-f

Borges, J. F., Bezzeghoud, M., Buforn, E., Pro, C., and Fitas, A. J. S. (2007). The 1980, 1997 and 1998 Azores earthquakes and some seismo-tectonic implications. *Tectonophysics* 435, 37–54. doi:10.1016/j.tecto.2007.01.008

Bott, M. (1959). The mechanics of oblique slip faulting. *Geol. Mag.* 96 (2), 109–117. doi:10.1017/S0016756800059987

Bougrine, A., Yelles Chaouche, A., and Calais, E. (2019). Active deformation in Algeria from continous GPS muserment. *Gephys. J. Int.* 2017, 572–588. doi:10.1093/GJI/GGZ035

Bounif, A., Bezzeghoud, M., Dorbath, L., Legrand, D., Deschamps, A., Rivera, L., et al. (2003). Seismic source study of the 1989, October 29, Chenoua (Algeria) earthquake from aftershocks, broad-band and strong motion records. *Ann. Geophys.* 46 (4), 625–646. doi:10.4401/ag-4370

Bounif, A., Dorbath, C., Ayadi, A., Meghraoui, M., Beldjoudi, H., Laouami, N., et al. (2004). The 21 May 2003 Zemmouri (Algeria) earthquake Mw 6.8: relocation and aftershock sequence analysis. *Geophys. Res. Lett.* 31, L19606. doi:10.1029/2004GL020586

Buforn, E. (2008). "Seismotectonics of Azores-Tunisia," in *The 1755 Lisbon earthquake revisited* Editors L. Mendes-Victor, C. Sousa Oliveira, J. Azevedo, and A. Ribeiro, 397–410.

Buforn, E., Bezzeghoud, M., Udias, A., and Pro, C. (2004). Seismic sources on the iberia-african plate boundary and their tectonic implications. *Pure Appl. Geophys.* 161 (3), 623–646. doi:10.1007/s00024-003-2466-1

Buforn, E., Sanz de Galdeano, C., and Udias, A. (1995). Seismotectonics of the ibero-maghrebian region. *Tectonophysics* 248, 247–261. doi:10.1016/0040-1951(94)00276-f

Buforn, E., Udias, A., and Colombas, M. A. (1988a). Seismicity, source mechanisms and tectonics of the Azores-Gibraltar plate boundary. *Tectonophysics* 152, 89–118. doi:10.1016/0040-1951(88)90031-5

Buforn, E., Udias, A., and Mezcua, J. (1988b). Seismicity and focal mechanisms in south Spain. *Bull. Seismol. Soc. Am.* 78, 2008–2224.

Buforn, E., Udías, A., and Pro, C. (2014). Large earthquakes at the Ibero-Maghrebian region: basis for an EEWS. *Pure Appl. Geophys* 172, 2387–2396. doi:10.1007/s00024-014-0954-0

Buforn, E., Udías, A., and Pro, C. (2016). Source mechanism studies of earthquakes in the Ibero-Maghrebian region and their tectonic implications. *J. Seismol.* 20, 1075–1088. doi:10.1007/s10950-015-9551-7

Caldeira, B., Fontiela, J., Borges, J. F., and Bezzeghoud, M. (2017). Grandes terremotos en Azores. *Física Tierra. ISSN-e* 29, 1988–2440. doi:10.5209/FITE.57601

Calvert, A., Gomez, F., Seber, D., Barazangi, M., Jabour, N., Ibenbrahim, A., et al. (1997). An integrated geophysical investigation of recent seismicity in the Al Hoceima Region of North Morocco. *Bull. Seism. Soc. Am.* 87, 637–651. doi:10.1785/bssa0870030637

Calvert, A., Sandvol, E., Seber, D., Barazangi, M., Roecker, S., Mourabit, T., et al. (2000). Geodynamic evolution of the lithosphere and upper mantle beneath the Alboran region of the western Mediterranean: constraints from travel time tomography. *J. Geophys. Res. Solid Earth* 105 (B5), 10871–10898. doi:10.1029/2000jb900024

Centroid Moment Tensor Project (Harvard CMT) (1976). On-line catalog. Available at: http://www.globalcmt.org/CMTsearch.html.

DeMetz, C., Gordon, R. G., Argus, D. F., and Stein, S. (1990). Current plate motions. *Geophys. J. Int.* 101 (2), 425–478. doi:10.1111/j.1365-246x.1990.tb06579.x

DeMetz, C., Gordon, R. G., Argus, D. F., and Stein, S. (1994). Effect of recent revisions to the geomagnetic reversal time scale on estimates of current plate motions. *Geophys. Res. Lett.* 21 (20), 2191–2194. doi:10.1029/94gl02118

De Vicente, G., Cloetingh, S., Munoz-Martin, A., Olaiz, A., Stich, D., Vegas, R., et al. (2008). Inversion of moment tensor focal mechanisms for active stresses around the micro-continent Iberia: tectonic implications. *Tectonics* 27, TC1009. doi:10.1029/2006TC002093

Dorbath, L., Hahou, Y., Delouis, B., Dorbath, C., Van Der Woerd, J., Bardrane, S., et al. (2005). "Etudes sismologiques sur le séisme D'Al Hoceima: localisation, et mécanisme du choc principal et des répliques, contraintes et structure de la zone épicentrale," in Communication, Colloque International Séisme d'Al Hoceima : bilan et perspectives, Al Hoceima, Morocco, February 2005, 24–26.

Dziewonski, A. M., Chou, T.-A., and Woodhouse, J. H. (1981). Determination of earthquake source parameters from waveform data for studies of global and regional seismicity. *J. Geophys. Res.* 86, 2825–2852. doi:10.1029/JB086iB04p02825

Ekström, G., Nettles, M., and Dziewonski, A. M. (2012). The global CMT project 2004-2010: centroid-moment tensors for 13,017 earthquakes. *Phys. Earth Planet. Inter.* 200-201, 1–9. doi:10.1016/j.pepi.2012.04.002

El, A. S., Tadili, B., Cherkaoui, T. E., Medina, F., Ramdani, M., Ait Brahim, L., et al. (1998). The Al Hoceima earthquake of May, 26, 1994 and its aftershocks: a seismotectonic study. *Ann. Geofis.* 41, 519–537. doi:10.4401/ag-3801

Fernández-Ibáñez, F., Soto, J. I., Zoback, M. D., and Morales, J. (2007). Present-day stress field in the Gibraltar Arc (western Mediterranean). *J. Geophys. Res. (Solid Earth)* 112, B08404. doi:10.1029/2006JB004683

Frohlich, C. (1992). Triangle diagrams: ternary graphs to display similarity and diversity of earthquake focal mechanisms. *Phys. Earth Planet. Inter.* 75, 193–198. doi:10.1016/0031-9201(92)90130-n

Geissler, W. H., Matias, L., Stich, D., Carrilho, F., Jokat, W., Monna, S., et al. (2010). Focal mechanisms for sub-crustal earthquakes in the Gulf of Cadiz from a dense OBS deployment. *Geophys. Res. Lett.* 37, L18309. doi:10.1029/2010GL044289

Gràcia, E., Grevemeyer, I., Bartolomé, R., Perea, H., Martínez-Loriente, S., Gómez de la Peña, L., et al. (2019). Earthquake crisis unveils the growth of an incipient continental fault system. *Nat. Commun.* 10, 3482. doi:10.1038/s41467-019-11064-5

Grimison, N. L., and Wang-Ping, C. (1986). The Azores-Gibraltar plate boundery: focal mechanisms, depth of earthquakes and their tectonic implications. *Journalo F. Geophys. esearch* 91 (B2), 2009–2047. Feb 0986. doi:10.1029/JB091iB02p02029

Gutscher, M. A., Dominguez, S., Westbrook, G. K., Le Roy, P., Ros, F., Duarte, J., et al. (2012). The Gibraltar subduction: a decade of new geophysical data. *Tectonophysics* 574–575, 72–91. doi:10.1016/j.tecto.2012.08.038

Harbi, A., Maouche, S., and Ayadi, A. (1999). Neotectonics and associate seismicity in the eastern tellian Atlas of Algeria. *J. Seismol.* 3 (1), 95–104. doi:10.1023/a:1009743404491

Hardebeck, J. L., and Hauksson, E. (2001). Stress orientations obtained from earthquake focal mechanisms: what are appropriate uncertainty estimate. *Bull. Seismol. Soc. Am.* 91 (2), 250–262. doi:10.1785/0120000032

Heidbach, O., Reinecker, J., Tingay, M., Müller, B., Sperner, B., Fuchs, K., et al. (2007). Plate boundary forces are not enough: second- and third-order stress patterns highlighted in the World Stress Map database. *Tectonics* 26. doi:10.1029/2007TC002133

Heidbach, O., Tingay, M., Barth, A., Reinecker, J., Kurfeß, D., and Müller, B. (2010). Global crustal stress pattern based on the World Stress Map database release 2008. *Tectonophysics* 482, 3–15. doi:10.1016/j.tecto.2009.07.023

INGV (2023). *Istituto Nazionale Geofisica e Vulcanologia (INGV)*. Available at: http://www.ingv.it/it/.

Instituto Geográfico Nacional (2023). Spanish seismic network (IGN). Available at: http://www.ign.es/ign/en/IGN/home.jsp.

International Seismological Centre (2020). On-line. *Bulletin*. doi:10.31905/D808B830

IRIS (Incorporated Researcher Institutions for Seismology) (2023). Incorporated researcher institutions for seismology. Available at: https://www.iris.edu/hq/.

Jiménez-Munt, I., Bird, P., and Fernandez, M. (2001). Thin-shell modeling of neotectonics in the Azores-Gibraltar region. *Geophys. Res. Lett.* 28 (6), 1083–1086. doi:10.1029/2000gl012319

Kostrov, V. V. (1974). Seismic moment and energy of earthquakes and seismic flow of rocks, Izv. *Acad. Sci. USSR, Phys. Solid Earth* 1, 23–40.

Koulali, A., Ouzar, D., Tahayt, A., King, R. W., Vernant, P., Reilinger, R. E., et al. (2011). New GPS constraints on active deformation along the Africa–Iberia plate boundary. *Earth Planet.* 308, 211–217. doi:10.1016/j.epsl.2011.05.048

Lentas, K., Di Giacomo, D., Harris, J., and Storchak, D. A. (2019). The ISC Bulletin as a comprehensive source of earthquake source mechanisms. *Earth Syst. Sci. Data* 11, 565–578. doi:10.5194/essd-11-565-2019

Lourenço, N., Miranda, J., Luis, J., Ribeiro, A., Mendes Victor, L. A., Madeira, J., et al. (1998). Morpho-tectonic analysis of Azores volcanic plateau from new bathymetric compilation of the area. *Mar. Geophys. Res.* 20, 141–156. doi:10.1023/A:1004505401547

Maouche, S., Meghraoui, M., Morhange, C., Belabbes, S., Bouhadad, Y., and Haddoum, H. (2011). Active coastal thrusting and folding, and uplift rate of the Sahel Anticline and Zemmouri earthquake area (Tell Atlas, Algeria). *Tectonophysics* 509, 69–80. doi:10.1016/j.tecto.2011.06.003

Martinez-Garcia, A., Rosell-Melé, A., Jaccard, S. L., Geiberte, W., Sigman, D. M., and Haug, G. H. (2011). Southern Ocean dust-climate coupling over the past four million years. *Nature* 476 (7360), 312–315. doi:10.1038/nature10310

McClusky, S., Reilinger, R., Mahmoud, S. B. S. D., and Tealeb, A. (2003). GPS constraints on Africa (Nubia) and Arabia plate motions. *Geophys. J. Int.* 155 (1), 126–138. doi:10.1046/j.1365-246X.2003.02023.x

Medina, F. (1995). Present-day state of stress in northern Morocco from focal mechanism analysis. *J. Struct. Geol.* 17, 1035–1046. doi:10.1016/0191-8141(94)00123-h

Meghraoui, M., Cisternas, A., and Philip, H. (1986). Seismotectonic of the lower chellif basin: structural background of the El Asnam (Algeria) earthquake. *Tectonics* 5 (6), 806–836. doi:10.1029/TC005i006p00809

Meghraoui, M., and Pondrelli, S. (2012). Active faulting and transpression tectonics along the plate boundary in North Africa. *Ann. Geophys* 55, 5. doi:10.4401/ag-4970

Michael, A. J. (1984). Determination of stress from slip data: faults and folds. *J. Geophys. Res. Solid Earth* 89 (B13), 11517–11526. doi:10.1029/jb089ib13p11517

Michael, J. A. (1987). Use of focal mechanisms to determine stress: a control study. *J. Geophys. Res.* 92, 357–368. doi:10.1029/jb092ib01p00357

Minster, J. B., and Jordan, T. H. (1978). Present-day plate motions. *J. Geophys. Res.* 83 (B11), 5331–5354. doi:10.1029/JB083iB11p05331

National Earthquake Information Center (NEIC) (2024). Earthquake. Available at: https://earthquake.usgs.gov.

Nocquet, J. M. (2012). Present-day kinematics of the Mediterranean: a comprehensive overview of GPS results. *Tectonophysics* 579 (0), 220–242. doi:10.1016/j.tecto.2012.03.037

Nocquet, J. M., and Calais, E. (2004). Geodetic measurements of crustal deformation in the western mediterranean and europe. *Pure Appl Geophys* 161, 661–681. 0033-4553/04/030661-21. doi:10.1007/s00024-003-2468-z

Ousadou, F., Dorbath, L., Ayadi, A., Dorbath, C., and Gharbi, S. (2014). Stress field variations along the Maghreb region derived from inversion of major seismic crisis fault plane solutions. *Tectonophysics* 632, 261–280. doi:10.1016/j.tecto.2014.06.017

Ousadou, F., Dorbath, L., Dorbath, C., Bounif, M. A., and Benhallou, H. (2013). The Constantine (Algeria) seismic sequence of 27 October 1985: a new rupture model from aftershock relocation, focal mechanisms, and stress tensors. *J. Seismol.* 17 (2), 207–222. doi:10.1007/s10950-012-9320-9

Ouyed, M., Meghraoui, M., Cisternas, A., Deschamps, A., Dorel, J., Frechet, J., et al. (1981). Seismotectonics of the El Asnam earthquake. *Nature* 292 (5818), 26–31. doi:10.1038/292026a0

Philip, H., and Meghraoui, M. (1983). Structural analysis and interpretation of the surface deformations of the El Asnam earthquake of October 10, 1980. *Tectonics* 2 (1), 17–49. doi:10.1029/TC002i001.P.00017

Piromallo, C., and Morelli, A. (2003). P wave tomography of the mantle under the Alpine-Mediterranean area. *J. Geophys. Res.* 108 (B2), 2065. doi:10.1029/2002JB001757

Platt, J. P., and Vissers, R. L. M. (1989). Extensional collapse of thickened continental lithosphere: a working hypothesis for the Alboran Sea and Gibraltar arc. *Geology* 17, 540–543. doi:10.1130/0091-7613(1989)017<0540:ecotcl>2.3.co;2

Pondrelli, S., Morelli, A., and Ekstrom, G. (2004). European-Mediterranean regional centroid-moment tensor catalog: solutions for years 2001 and 2002. *Phys. Earth Plan. Int.* 145 (1-4), 127–147. doi:10.1016/j.pepi.2004.03.008

Pondrelli, S., Salimbeni, S., Morelli, A., Ekström, G., and Boschi, E. (2007). European-mediterranean regional centroid moment tensor catalog: solutions for years 2003 and 2004. *Phys. Earth Planet. Int.* 164 (1-2), 90–112. doi:10.1016/j.pepi.2007.05.004

Pondrelli, S., Salimbeni, S., Morelli, A., Ekström, G., Postpischl, L., Vannucci, G., et al. (2011). European-mediterranean regional centroid moment tensor catalog: solutions for 2005-2008. *Phys. Earth Planet. Int.* 185 (3-4), pp74–81. doi:10.1016/j.pepi.2011.01.007

QAFI (2023). Quafi quaternary active faults in Iberia. Available at: http://info.igme.es/qafi/.

Rebaï, S., Philip, H., and Taboada, A. (1992). Modern tectonic stress field in the Mediterranean region: evidence for variation in stress directions at different scales. *Geophys. J. Int.* 110, 106–140. doi:10.1111/j.1365-246x.1992.tb00717.x

Seber, D., Barazangi, M., Ibenbrahim, A., and Delati, A. (1996). Geophysical evidence for lithospheric delamination beneath the Alboran Sea and Rif-Betic mountains. *Nature* 379, 785–790. Feb 1996. doi:10.1038/379785a0

Sella, G. F., Dixon, T. H., and Mao, A. (2002). REVEL: a model for Recent plate velocities from space geodesy. *J. Geophys. Res. Solid Earth* 107 (B4), ETG 11–30. doi:10.1029/2000JB000033

Serpelloni, E., Vannucci, G., Pondrelli, S., Argnani, A., Casula, G., Anzidei, M., et al. (2007). Kinematics of the western Africa–Eurasia plate boundary from focal mechanisms and GPS data. *Geophys. J. Int.* 169 (3), 1180–1200. doi:10.1111/j.1365-246X.2007.03367.x

Sïdi, A., Chardon, D., Baby, P., and Ouali, J. (2011). Active oblique ramp faulting in the southern Tunisian Atlas. *Tectonophysics* 499 (1), 178–189. doi:10.1016/j.tecto.2011.01.010

Soumaya, A., Ben Ayed, N., Delvaux, D., and Ghanmi, M. (2015). Spatial variation of present-day stress field and tectonic regime in Tunisia and surroundings from formal inversion of focal mechanisms: geodynamic implications for central Mediterranean. *Tectonics* 33, 1154–1180. doi:10.1002/2015TC003895

Soumaya, A., Ben Ayed, N., Rajabi, M., Meghraoui, M., Delvaux, D., Kadri, A., et al. (2018). Active faulting geometry and stress pattern near complex strike-slip systems along the Maghreb region: constraints on active convergence in the western Mediterranean. *Tectonics* 37, 3148–3173. doi:10.1029/2018TC004983

Stich, D., Mancilla, F. L., Baumont, D., and Morales, J. (2005). Source analysis of the M_w 6.3 2004 Al Hoceima earthquake (Morocco) using regional apparent source time functions. *J. Geophys. Res.* 110. doi:10.1029/2004JB003366

Swezey, C. S. (1996). Structural controls on Quaternary depocentres within the Chotts Trough region of southern Tunisia. *J. Afr. Earth Sci.* 22 (3), 335–347. doi:10.1016/0899-5362(96)00012-7

Swiss Seismological Service (2024a). Eidgenössische technische hochschule zürich (ETHZ). Available at: www.seismo.ethz.ch/.

Swiss Seismological Service (2024b). Zurich moment tensors (ZUR_RMT). Available at: http://www.seismo.ethz.ch.

Van der Woerd, J., Dorbath, C., Ousadou, F., Dorbath, L., Delouis, B., Jacques, E., et al. (2014). The Al Hoceima Mw 6.4 earthquake of 24 February 2004 and its aftershocks sequence. *J. Geodyn.* 77, 89–109. doi:10.1016/j.jog.2013.12.004

Vannucci, G., Pondrelli, S., Argnani, A., Morelli, A., Gasperini, P., and Boschi, E. (2004). An Atlas of mediterranean seismicity. *Ann. Geophys.* 47 (1), 247–302. doi:10.4401/ag-3276

Watts, A. B., Platt, J. P., and Buhl, P. (1993). Tectonic evolution of the Alboran Sea basin. *Basin Res.* 5, 153–177. doi:10.1111/j.1365-2117.1993.tb00063.x